Study on roll damping around a circular cylinder

S.H. Kwon[1], L. Lu[2], X. Chen[3*], B.J. Kim[1], S.C Jiang[2], S.Y. Han[1], J.T.Do[1], K.S. Ahn[1], D. Ren[1]

[1]Department of Naval Arch. and Ocean Eng., Pusan National University, Busan, Korea
[2]Center for Deep Water Engineering, Dalian University of Technology, Dalian 116024, China
[3]Deep water Technology Research Centre(DTRC), Bureau Veritas, HarbourFront Centre, Singapore
E-mail: shkwon@pusan.ac.kr

Rolling of a half-immersed circular cylinder on the free surface is studied in order to analyze roll damping due to *unique* effect of fluid viscosity. The damping moments due to fluid friction, fluid velocity vector around the cylinder and free-surface elevations are measured in model tests. Numerical computations based on 2D Navier-Stokes solver with free surface and empirical formula by ignoring free-surface effect are performed.

1. Introduction

The estimation of roll damping remains to be one of the research areas challenging to naval architects and ocean engineers. The present study is motivated by the desire to separate the damping due to viscosity and that due to radiation on the free surface. As a result one can test numerical code which calculates viscous effect. In order to achieve this purpose, the circular cylinder is rotated around cylinder center. Since the center of rotation is located at the center of the cylinder, the potential code will not be able to calculate any disturbance while the viscous code can calculate shear stress component alone. In the model tests, the roll angle is kept fixed as 5 degree. The circular cylinder is rotated at various frequencies ranging from 0.29 to 2.56 Hz. The moment to drive rolling is measured by piezoelectric type load cell. The flow fields are measured by PIV measuring system. Numerical analysis was carried out by solving 2 dimensional Navier-Stokes equations. VOF technique was used to capture the free surface. Furthermore, an empirical formula by neglecting free-surface effect has been derived based on the formula of oscillating laminar boundary layer. Experimental measurements are compared with those of numerical analysis and empirical formula.

2. Experimental measurements

The total number of test cases is twenty-five cases. The non-dimensional frequency $\omega\sqrt{D/2g}$ varies from 0.25 to 2.15 with constant increment 0.05. Thirteen cases are tested with Particle Image Velocimetry (PIV) and the results are analyzed. The shape and dimension of model are shown in Fig 1. The roll motion belongs to the y-z plane. The positive x-direction is along the axial direction of the circular cylinder. The 31.2m long wave flume is used for this experiment. The length between the location of the model and wave absorber is 9.7m and the wave gauge is located 3m away from the model. The model position and gauge set-up position is shown in Fig. 2. The dimension of the model is 590mm (L)$\times$ 350mm (D)$\times$ 175mm (d). The water depth was 710mm.
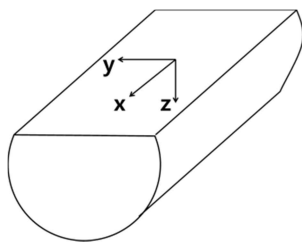

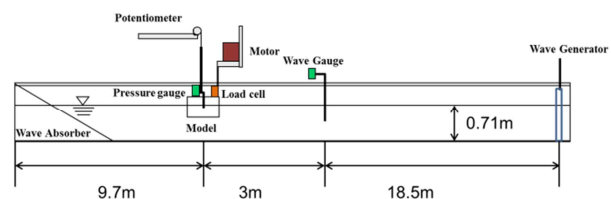Fig. 1 Model & Reference coordinate system

Fig. 2 Schematic view of the wave flume and model set-up
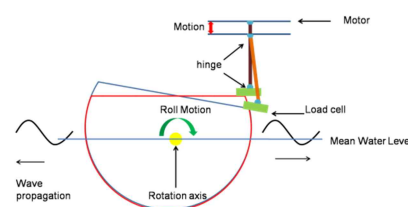

Fig. 3 Load cell

Fig. 4 Driving mechanism of roll motion

Apparatus

In this experiment, potentiometer, load cell, and wave gauge were used to measure the motion amplitude, forces in three axis, and wave elevation, respectively. The load cell measures the forces in three axis and the calibrated ranges of x, y are from 0 to 1kN and that of z is from 0 to 8kN. The load cell is shown in Fig. 3. The driving mechanism of the forced roll motion is shown in Fig. 4.

Force and Moment time series

The forces in three directions are presented in Fig. 5. The force in the x-direction is shown in Fig. 5(a). Since the force in the x-direction is independent of the roll motion, there shouldn't be force component in this direction. However, there is small oscillating force since the connection between the jig and test model is not exactly perpendicular. The force in y-direction is positive when the model is pressed. Since the pulling force is lower than pressing force, the amplitude in positive direction is bigger than that in negative direction. Unlike the forces in y and z-direction, the roll moment shows clearly sinusoidal time series as seen in Fig 6. However, for relatively long excitation period cases, roll moment does not show a clear sinusoidal shape, since the force in z-direction has small amplitude.

PIV

Using PIV, the velocity vector field is visualized. Vorticity contoured is presented. Total 13 cases are examined. The velocity vector fields are visualized at the each quarter of the period. The significant velocity vector and the vorticity are confined near to the free surface for all the cases. Small portion of vorticity can be found near to the cylinder surface as shown in Fig. 7. It means that irrotational flow assumption can be valid away from the free surface and body surface. This visualization clearly shows that there is viscosity damping due to shear stress even when the center of rotation is located at the center of the cylinder.
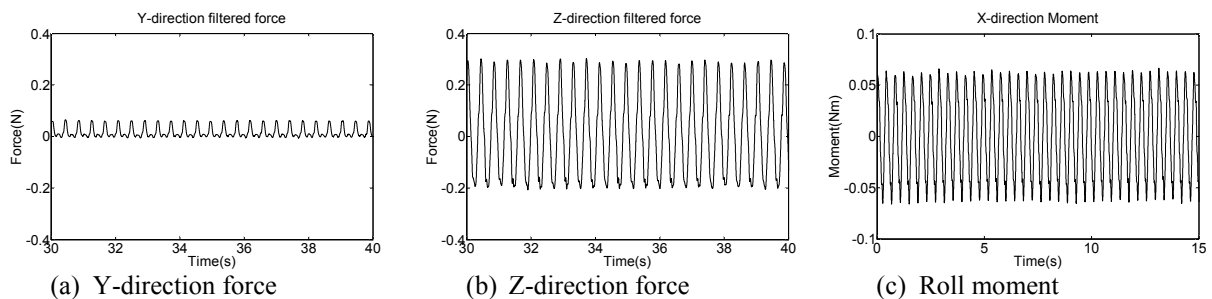

(a) Y-direction force (b) Z-direction force (c) Roll moment

Fig. 5 Forces and Moment Time history for oscillatory period T=0.41s

(a) Y-direction force (b) Z-direction force (c) Roll moment
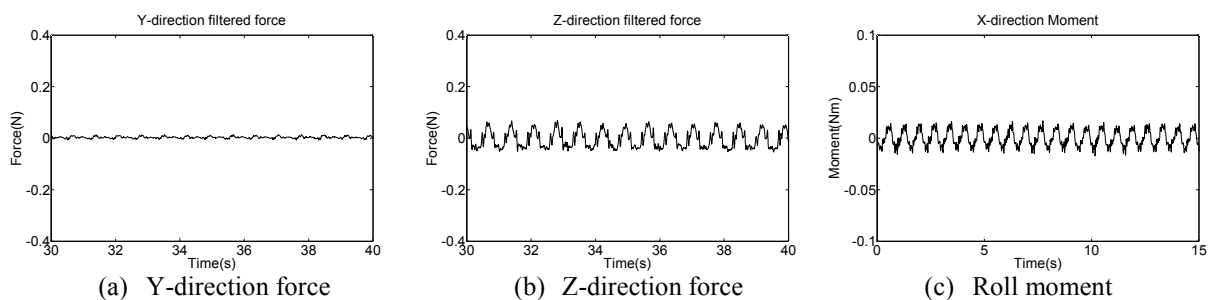
Fig. 6 Forces and Moment Time history for oscillatory period T=0.71s

(a) t/T=0 (b) t/T=0.25 (c) t/T=0.50 (d) t/T=0.75
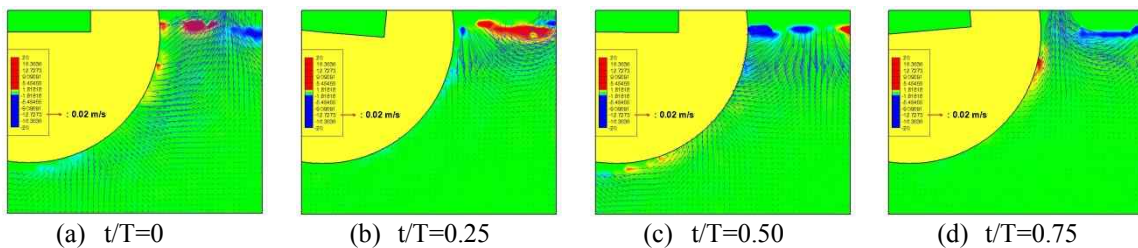
Fig.7 PIV analysis at oscillatory period T=0.41s

Wave elevation

(a) T = 0.41s (b) T = 0.71s
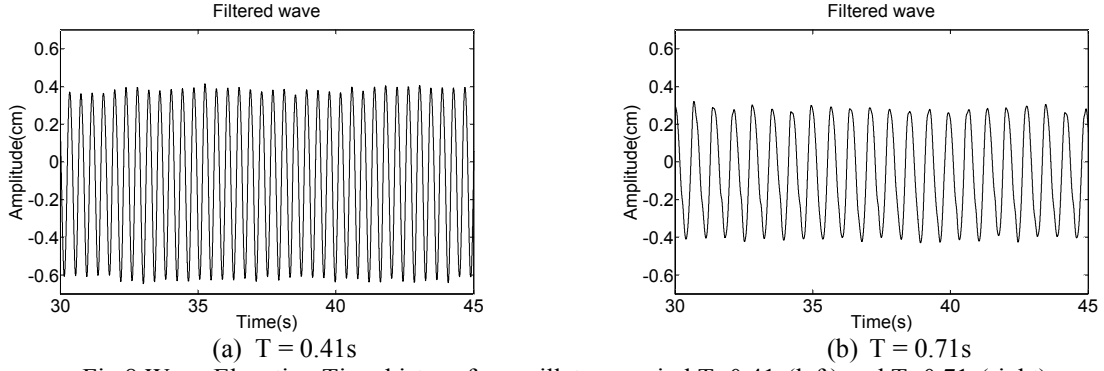
Fig.8 Wave Elevation Time history for oscillatory period T=0.41s(left) and T=0.71s(right)

The measured wave elevation is illustrated in Fig. 8. The wave generated from high frequency cylinder motion shows higher wave height due to its higher kinetic energy.

3. Empirical analysis for a cylinder in infinite fluid

By ignoring free surface effect, the shear stress on the cylinder surface can be evaluated by the formula for oscillating boundary layer (Jensen et al., 1989; Lu and Chen, 2012)

$$\tau = -\frac{1}{2}\rho C_f |V_\tau| V_\tau$$

where τ is the shear stress per unit area, ρ the water density, C_f and V_τ are the frictional coefficient and tangent velocity component, respectively, with $V_\tau = R\dot{\theta}$, $\theta = \theta_0 \cos(\omega t)$, $C_f = 2/\sqrt{Re}$, $Re = aV_\tau^a/v$, $a = R\theta_0$. Note that the notation of a and V_τ^a are the amplitudes of rotation and tangent velocity, respectively. Thus we have $\tau = -\rho\sqrt{v}R\theta_0\omega^{3/2} |\sin(\omega t)| \sin(\omega t)$, and the total moment exerts on the rotary oscillating cylinder from the water reads

$$M = \int_0^\pi \tau(Rd\theta) \cdot L \cdot R = -\pi\rho\sqrt{v}R^3 L\theta_0\omega^{3/2} |\sin(\omega t)| \sin(\omega t)$$

where L = 0.57m is the length of the cylinder used for the experiments. Accordingly, the amplitude of the roll moment expression is

$$M^a = -\pi\rho\sqrt{v}R^3\theta_0 L\omega^{3/2}\frac{8}{3\pi}$$

For the typical cases with oscillating periods of 0.71s and 0.41s, the above equation leads to the amplitudes of the moment being 0.019 and 0.044 Nm, respectively.

4. CFD simulations

In accordance to the experimental set-up, two dimensional numerical simulations based on the Navier-Stokes equation by using OpenFoam package were conducted. The free surface is captured by a VOF technique. In order to accurately compute the large velocity gradient in the boundary layer, very fine computational grid is used in the vicinity of the cylinder. The first layer of mesh consists of 360 uniform cells with a height of D/150, giving nearly 200,000 meshes in the computational domain. The numerical computation can be regarded as a two dimensional Direct Numerical Simulation with high grid resolution. Fig. 9 (a) and Fig. 8 (b) present two typical time-series of moments for the cases with T = 0.41s and 0.71s, respectively. The moment amplitudes observed from Fig. 8 are close to 0.035Nm and 0.02Nm, respectively, which are reasonably close to the experimental data and empirical predictions. All the results are summarized in Table 1.
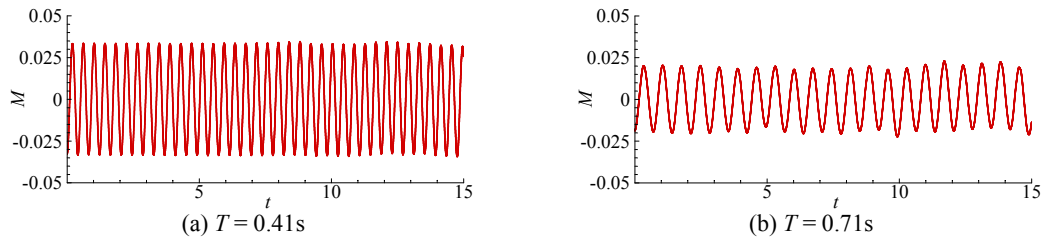
(a) $T = 0.41$s

(b) $T = 0.71$s

Fig. 9 Roll moment time history for oscillatory period T=0.41s(left) and T=0.71s(right)

Table. 1 Comparison of roll moment amplitudes

Roll period (s)	Experiment (Nm)	Numerical analysis (Nm)	Empirical formula (Nm)
0.41	0.062	0.035	0.044
0.71	0.014	0.020	0.019

Fig. 10 shows the vorticity and velocity vectors around the rotational circular cylinder for the case with T=0.41s. The CFD numerical results provide more details of the flow. It is found that attached vortices are developed on both sides of the cylinders, and the flow pattern varies little with the time development. The most significant vortices appear along the free surface, which is consistent with the experimental observations as shown on Fig. 7. The absence of the attached vortex in Fig. 7 is attributed to the relatively low resolution of PIV compared with the CFD simulations. It is expected that the near region of free surface involves most of the mechanical energy dissipation.
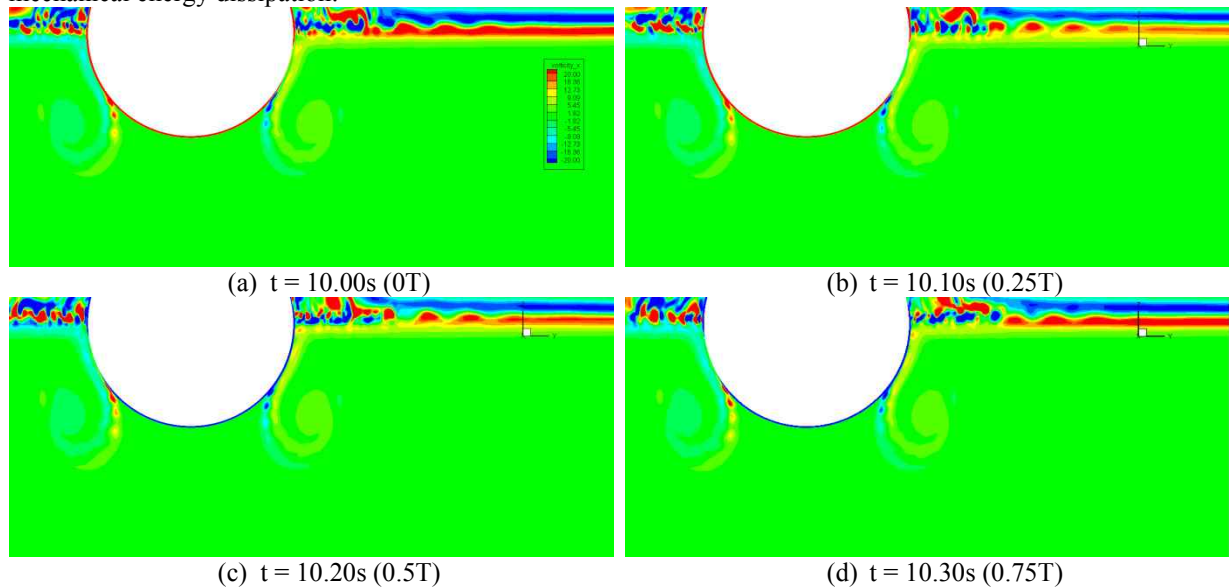

(a) t = 10.00s (0T)

(b) t = 10.10s (0.25T)

(c) t = 10.20s (0.5T)

(d) t = 10.30s (0.75T)

Fig. 10 Vorticity and velocity vector for the case with T = 0.41s

References

L. Bonfiglio, S. Brizzolara, C. Chryssostomidis, 2012, "Added Mass and Damping of Oscillating Bodies: a fully viscous numerical approach", *Recent Advances in Fluid Mechanics, Heat & Mass Transfer and Biology*

B.L. Jensen, B.M. Sumer and J. Fredsoe, 1989, "Turbulent oscillatory boundary layers at high Reynolds numbers". *Journal of Fluid Mechanics*, 206, 265-297.

L. Lu, X.B., Chen, 2012, "Dissipation in the gap resonance between two bodies". Proc. 27th IWWWFB conference,22-25, April, Copenhagen(Denmark).

Rae H. Yuck, Dong H. Lee, Hang S. Choi, 2003, "A Study on Roll Damping of 2-D Cylinders", *International Journal of Offshore and Polar Engineering*, Vol. 13, No. 3